Dentistry 3000

Vol 14, No 3 (2026)
ISSN 2167-8677 (online)
DOI 10.5195/d3000.2026.1665

Cold Challenge Transillumination Laser Speckle Contrast Imaging of Pulpal Microvascular Recovery for Differentiating Reversible from Symptomatic Irreversible Pulpitis

A Prospective Blinded Diagnostic Study

Ahmed Laith Salman Azzawi[1], Hasan Nabeel Abdulqadeer[1], Omar Faez Abdulateef[2]
[1]College of Dentistry, Uruk Universit, Baghdad, Iraq
[2]College of Dentistry, Al-Farahidi University, Baghdad, Iraq

Abstract

In the present prospective, blinded, diagnostic study, the authors sought to assess the ability of cold challenge transillumination laser speckle contrast imaging (LSCI) to discriminate between reversible pulpitis (RP) and symptomatic irreversible pulpitis (SIP) based on the amount of microvascular recovery following the cold challenge. A total of 50 adults were selected with mature permanent molars with deep caries (25 RP and 25 SIP cases). The continuous LSCI recording consisted of a 20 s baseline, a standardized 5 s cold challenge and 180 s for recovery. A significant diagnosis-by-time interaction was found using mixed-effects analysis, with the largest difference at ~60 seconds and convergence at ~180 seconds. The LSCI index of recovery had an AUC of 0.9088, a sensitivity of 72%, a specificity of 96%, and a positive likelihood ratio of 18.0. Cold-response duration attained an AUC of 0.8528 while EPT presented with a low discrimination (AUC 0.6056). The addition of LSCI to the conventional model improved the AUC from 0.8704 to 0.9568 (p=0.0438). A positive correlation was seen between the recovery index and the severity of the histopathology (Spearman ρ=0.551, p=0.00788) for the 22 cases of SIP that underwent histology. Inter-analyst reproducibility was excellent (ICC=0.993) with 92% of RP teeth having 6-month confirmation. Thus, cold challenge transillumination LSCI showed potential as a physiologic approach for discriminating RP from SIP and as a complementary diagnostic tool to conventional sensibility testing. These results suggest that recovery kinetics, and not baseline perfusion alone, may reflect clinically relevant vascular dysfunction with increasing pulpal inflammation while retaining a noninvasive, tooth-specific approach to assessment.

Open Access

Citation: Azzawi ALS et al. (2026) Cold Challenge Transillumination Laser Speckle Contrast Imaging of Pulpal Microvascular Recovery for Differentiating Reversible from Symptomatic Irreversible Pulpitis. Dentistry 3000. 1:a001 doi:10.5195/d3000.2026.1665
Received: October 18, 2026
Accepted: November 1, 2026
Published: November 18, 2026
Copyright: ©2026 Azzawi ALS et al. This is an open access article licensed under a Creative Commons Attribution Work 4.0 United States License
Email: ahmed.I.salman@uruk.edu.iq

Introduction

Characterization of pulpal inflammation is an important aspect of endodontic decision making today, as the biological status of the pulp can exist along a continuum that does not always fit into the traditional categories. Recent clinical validation of alternative pulpitis classifications has shown that discrimination between disease phenotypes is improved by stratifying them into mild, moderate, and severe pulpal inflammatory states, suggesting that approaches that reflect the actual severity and biological behavior of pulpal inflammation rather than symptom-based categories are needed [1].

Reversible and symptomatic irreversible pulpitis has become more relevant with the change in management which recommended preservation of vital pulp tissues. Current evidence suggests that even older permanent teeth with clinical findings typical of irreversible pulpitis, may have sufficient healing potential to support vital pulp therapy if the biological and clinical conditions are right. Therefore, the accurate determination of the inflammatory status of the pulp is becoming more relevant in the diagnosis and in the decision

New articles in this journal are licensed under a Creative Commons Attribution 4.0 United States License.

This journal is published by Pitt Open Library Publishing.

between pulp-preserving and conventional root-canal treatment techniques [2].

The traditional methods of diagnosing pulpitis are still largely based on the patient's complaint of pain, clinical examination, interpretation of dental radiographs, thermal stimulation, and electric pulp testing. These procedures offer valuable clinical data and may be limited in their ability to accurately reflect the actual inflammatory status of the contained pulp tissue. The availability of diagnostic literature remains heterogenous and well-designed clinical studies directly verifying the diagnostic finding regarding the biological situation of the pulp is comparatively limited, which means that the relation between the common clinical categories and the tissues is not quite clear [3].

The clinical and radiographic features are not always related to the histopathologic extent of pulpal inflammation. There is a marked difference in inflammatory-cell infiltration, vascular changes, tissue disorganization, and necrosis in human molars classified clinically as reversible and irreversible pulpitis, and there is not a complete correlation between the clinical diagnosis and the microscopic tissue status. The clinicopathologic variability would argue that objective physiological measurements that reflect tissue behavior before irreversible treatment decisions are made are warranted [4].

The inflammatory and neuroimmune microenvironment responds to progression of reversible to symptomatic irreversible pulpitis with discernible changes. In symptomatic irreversible pulpitis, there is increased neutrophilic infiltration and evidence of neutrophil extracellular-trap formation as well as changes in cellular components involved in pulpal neuroimmune regulation. The results of this study suggest that pulpitis at the clinicopathological level is associated with detectable tissue changes and confirm the biological validity of pursuing diagnostic techniques that are sensitive to physiologic consequences of inflammation in addition to neural perception [5].

Irreversible pulpitis is also linked to a unique inflammatory environment and is additionally shown by molecular evidence. It has been shown that mediators such as tumor necrosis factor-α, interleukin-2, interleukin-6, interleukin-8, substance P, calcitonin gene-related peptide and catalase are increased in expression in symptomatic irreversible pulpitis compared to healthy pulp. Interestingly, there may also be inflammatory activity in teeth with similar or less pain activity, and pain alone cannot be assumed to reflect the whole biology of pulp activity [6].

Objective biomarkers are an emerging pulpal diagnostic tool, then. Over 70 molecular targets have been studied associated with pulpal health and inflammation, some of which have demonstrated potentially useful diagnostic characteristics in some comparisons, for example, interleukin-6 and interleukin-8. However, methodological heterogeneity, small sample sizes, the lack of a universally accepted diagnostic reference standard and the inability of many markers to distinguish pulpitis stages with clinical relevance is a limitation of the overall certainty of the evidence [7].

The inflammatory information of pulpitis itself exists in the pulpal blood, which can differentiate clinically relevant pulpitis phenotypes. Interleukin-8 has been found to have high separation of reversible and irreversible pulpitis (up to an area under the curve of 1.0), and the separation for tumor necrosis factor-α has been found to be moderate. The results agree with the concept that objective biological parameters can be used in conjunction with symptoms to diagnose the disease, but that blood sampling is not a non-invasive pre-operative diagnostic tool as it provides pulpal exposure [8].

Other cytokine profiles also indicate that there are progressive biological changes between normal pulp, reversible pulpitis, and symptomatic irreversible pulpitis. The concentration of interleukin-4, interleukin-5, interleukin-10 and interleukin-13 in pulps are increased with inflammatory disease, and the combined analysis of these T-helper-2-associated cytokines had an area under the receiver operating characteristic curve of around 0.90, discriminating between irreversible and reversible pulpitis. These observations again argue for the presence of quantifiable biological transitions between conventional diagnostic categories [9].

Another possibility for quick objective evaluation is point-of-care analysis of pulpal blood. Clinical data are available and preliminary analyses show a strong association between inflammatory pain intensity and high sensitivity C-reactive protein measured during pulpal access, which has high discriminatory performance in the identification of high symptomatic phenotypes. The invasiveness of the collection of pulpal blood, however, and the small size of the initial cohorts of patients that might be diagnosed using these methods, underscore the continued importance of developing non-invasive approaches to physiologic assessment that may be able to detect pulpal disease in an early stage without the need for operative exposure [10].

Pulp vitality is primarily vascular in nature, while the usual pulp tests involving cold and electric pulp sensory responsiveness. Meta-analytic comparisons of these different methods have demonstrated significantly better diagnostic accuracy for a method of vitality that relies on blood flow, such as pulse oximetry, over electric sensibility, cold sensibility, and heat sensibility testing, but quality of the available studies is limited. This is crucial, since maintaining neural responsiveness does not necessarily reflect the extent of inflammatory vascular dysfunction in a living pulp [11].

Search for direct and non-invasive indicators of pulp vitality has therefore extended beyond the traditional methods of thermal and electrical stimulation. Different experimental modalities, such as optical methods, Doppler-based techniques, magnetic resonance approaches, ultrasound flowmetry, thermometric methods, terahertz technologies, and others have been investigated to find biological features more closely related to pulp perfusion and vitality. Optical methods are also appealing as they could, at least in principle, be used to interrogate vascular behavior without exposing the pulp, and with technical standardization and clinical validation prior to widespread use [12].

The circulation in the pulp is not fixed, and it is subject to dynamic responses to thermal stimulation. A decrease in pulpal circulatory signal after controlled cooling of the tooth and a recovery to baseline after the stimulus was removed has been observed in optical monitoring of healthy human teeth. This capacity to observe the disturbance and recovery allows for the possibility that the temporal vascular response to a standard thermal challenge may also contain information of physiological interest that is not available from a single measurement at rest, and it provides a basis for determining the time course of recovery from the cold challenge [13].

Laser speckle imaging is another optical approach used for perfusion detection that is based on the fluctuation of coherent-light interference patterns generated by incoherent moving scatterers, such as erythrocytes. Transillumination geometry has been able to differentiate between the presence and absence of simulated pulpal flow in dental models and has been found to be more suitable for interrogation of the pulp chamber than surface epi-illumination. This technique provides thus a physical method for quick and contactless evaluation of relative perfusion via the mineralized tooth structure [14].

More recent laser speckle contrast imaging findings have verified that the speckle flow index can respond quantitatively to controlled changes in simulated pulpal blood-flow velocity and have shown that optical parameters like dentin thickness can affect the measured signal. This is a hint for within-tooth normalization and dynamic measurements to minimize the impact of interindividual optical variability. Based on this, in the present study cold challenge transillumination laser speckle contrast imaging was assessed as a physiologic method to differentiate between reversible pulpitis and symptomatic irreversible pulpitis by

characterizing the magnitude and persistence of vascular disturbance, recovery timing and an integrated microvascular recovery index, and compared its diagnostic contribution to conventional sensibility testing, and related it to the histopathologic severity [15].

The purpose of this study was to determine if the dynamic recovery of pulpal microvascular flow following a standardized thermal stimulus, as measured by cold-challenge transillumination laser speckle contrast imaging, could differentiate between the two types of pulpal pathology, reversible pulpitis and symptomatic irreversible pulpitis. The study was intended to go beyond the traditional sensibility testing procedures, which are essentially a measure of neural responsiveness, and to examine a physiologic parameter more directly related to pulpal vascular behavior and tissue vitality.

The specific objectives of the study were to describe the temporal pattern of pulpal microvascular response to cold before, during, and following cold stimulation and whether there was a difference in the normalized speckle-flow recovery curve between teeth with reversible pulpitis and those with symptomatic irreversible pulpitis. Physiologic parameters coming from the recovery curve were emphasized such as immediate percentage change from baseline, post-challenge nadir or peak, time to 50% and 90% recovery, recovery slope, and area under the normalized recovery curve.

The main aim was to assess the diagnostic accuracy of a prespecified microvascular recovery index for the differentiation of symptomatic irreversible pulpitis and reversible pulpitis. The receiver operating characteristic curve and its area under the curve were estimated to examine diagnostic accuracy, along with the sensitivity, specificity and likelihood ratios derived from a user-defined diagnostic threshold. The study also sought to compare the diagnostic information that the microvascular recovery variables obtained by the laser-speckle method yielded with that obtained by conventional clinical tests of the pulp, such as the cold-response duration and the electric pulp-testing threshold. Importantly, the incremental diagnostic value of the dynamic vascular index was then assessed to assess if the physiologic imaging approach gave any discriminatory information aside from the routinely used sensibility-based approaches.

A second aim was to analyze the time course of the recovery of pulpal blood-flow for the entire post-challenge observation period and to evaluate if the recovery course of the vascular response was different between the two diagnostic groups. The purpose of this analysis was to determine if the general shape and the timing of the recovery response, not just a single, static measurement, reflected group separation.

The study also aimed at exploring the correlation between laser-speckle-derived microvascular characteristics and histopathologic severity of the pulpal inflammation in the teeth undergoing pulpal extraction as part of the planned treatment. The aim of this comparison was to see if there was correlation between the vascular recovery changes and inflammatory infiltration, vascular congestion, necrosis, formation of microabscesses, or other histopathologic evidence of the severity of pulpal disease.

Lastly, the study was designed to examine the validity and reproducibility of the laser speckle imaging procedure, including variability in signal quality, within-sequence variability, and inter-analyst variability when processing the images and extracting the region of interest. Teeth originally diagnosed as reversible pulpitis were followed up as well to verify maintenance of vitality and resolution of signs and symptoms for further reinforcing the clinical reference classification for diagnostic evaluation.

Material and Methods

Study Design and Diagnostic Framework

The study was a prospective, assessor-blinded, two-group physiologic diagnostic-accuracy investigation to evaluate the ability of the dynamic pulpal microvascular response to a standardized cold challenge to differentiate reversible pulpitis from symptomatic irreversible pulpitis in mature permanent molars. The index test comprised transillumination laser speckle contrast imaging (LSCI) that was carried out continuously before and after a controlled thermal challenge, while the target condition was the adjudicated pulpal diagnosis. To make the acquisition and processing of the LSCI signal independent of the final reference classification, the diagnostic pathway was designed that way. A reference diagnosis was separately determined by combining the pretreatment clinical phenotype, the findings of definitive treatment, the available histopathologic findings, and chronological clinical follow-up. The study was reported in accordance with the standards of STARD 2015 for diagnostic-accuracy studies (specifically, participant selection, index testing, reference standards, masking, and diagnostic-accuracy analysis).

One index tooth of an individual was taken as the unit of analysis. Video frames (or repeated speckle measurements) and serial post-challenge observations were never considered as statistically independent experimental units and were treated as repeated observations nested within the same tooth. The experimental hypothesis was that reversible and symptomatic irreversible pulpitis would be differences of quantitative and temporal aspects of the vascular disturbance produced by cold, and not merely in the presence or absence of pulpal blood flow.

Study Setting and Participant Recruitment

Adults with deep carious lesions on mature permanent first or second molars were recruited from the endodontic clinical service in a prospective manner. Consecutive potentially eligible patients were screened against the predefined eligibility criteria (clinical, radiographic, and optical imaging) until the prespecified balanced sample had been completed. A fixed total sample of 50 participants was obtained by stopping enrollment when 25 evaluable participants were included in the reversible-pulpitis group and 25 evaluable participants were included in the symptomatic-irreversible-pulpitis group.

One tooth was enrolled from participants. When more than 1 tooth was potentially eligible for selection, the tooth causing the presenting symptoms and meeting all the diagnostic criteria was selected. Recruitment, conventional clinical testing, LSCI acquisition, definitive treatment and reference-standard adjudication were kept as separate procedural steps to prevent knowledge gained in a later step influencing acquisition of the index test.

Eligibility Criteria and Tooth Selection

Eligible for inclusion were adults 18 years or older with a mature permanent first or second molar with a radiographically closed apex, deep caries reaching the pulp and a positive sensibility test when baseline assessment was made. Teeth had to meet the following clinical criteria: the clinical phenotype had to be either reversible pulpitis or symptomatic irreversible pulpitis, and a reproducible optical access to both the buccal and the lingual side of the crown had to be possible.

Teeth were excluded if they had previously been treated with root-canal treatment, pulpotomy, pulpectomy, or any other type of endodontic treatment; if the tooth apex was immature; if external root resorption, internal root resorption, vertical root fracture, an unrestorable crown, or extensive periapical disease was present, and if extensive periapical disease did not match the comparison of two vital-pulp conditions. Teeth with clinical and/or radiographic findings suggestive of total pulp necrosis were not used. Additionally full-coverage crowns, wide-spaced opaque metal restorations that would block the intended transillumination pathway, or structural defects that prevented appropriate optical acquisition were excluded as these could have a material effect on light transmission. Technically non-evaluable teeth were those for which a stable silicone index could not be obtained or for which a

movement-free optical imaging could not be achieved.

Diagnostic Group Definition and Baseline Pulpal Classification

Baseline pulpal classification was made prior to the LSCI results. Reversible pulpitis was diagnosed as a vital inflamed pulp with clinical signs or symptoms that suggested inflammation would subside after the removal or control of the etiologic stimulus. In this group, the teeth presented with stimulus dependent symptoms, no history of pulpal pain that was spontaneous or at night and their cold response would subside promptly after the stimulus was removed and would not persist as seen in symptomatic irreversible disease.

Irreversible pulpitis was classified as symptomatic and defined as a vital inflamed pulp for which spontaneous resolution could not be predicted, based on the conventional clinical phenotype. Qualifying characteristics included familiar severe thermal pain, lasting longer than the cold stimulus (usually 30 seconds or more), spontaneous pain, referred pain, nocturnal pain, or a combination of these. These definitions were like those published by the American Association of Endodontists, which included reversible pulpitis as inflammation which is expected to heal and symptomatic irreversible pulpitis as an inflamed pulp which is not likely to heal and in which thermal, spontaneous or referred pain is a characteristic descriptor.

The baseline classification was assumed to be a clinical phenotype and not the ultimate reference-standard diagnosis. This was preserved because clinical symptoms and sensibility responses were understood to be incomplete indicators of the state of the underlying histopathology of the pulp.

Preoperative Clinical and Radiographic Assessment

Standardized history taken prior to local anesthesia or surgical procedure. They asked the participant about the onset, duration, frequency, intensity, site of the presenting pain, and factors that provoked the pain, focusing upon the following: spontaneous pain, lingering thermal discomfort in the area, awakening at night due to pain, pain spreading to other areas, worsening of pain with different postures, chewing discomfort, and recent analgesic use. The affected tooth and surrounding teeth were examined for caries, dental restoration, crack, fracture, discoloration, swelling, sinus tract, and periodontal abnormalities. The teeth were palpated and axially and laterally percussed and compared to a clinically normal contralateral or adjacent control tooth if one was available.

A digital periapical radiograph taken with a paralleling technique before surgery was analyzed for caries depth, proximity of the lesion to the pulp chamber, morphology of the pulp chamber and root-canal, apical maturation, periodontal-ligament width, integrity of lamina-dura, periapical radiolucency, calcification, resorption, previous endodontic treatment, and root fracture. Radiography was employed as a parameter to determine eligibility and as a parameter to identify disease that would be contradictory to the planned vital-pulp comparison and not directly as a measure of pulpal blood flow.

Standardized Cold-Challenge Protocol

The experimental vascular challenge was conducted in addition to the traditional diagnostic cold test. The dental refrigerant spray, HYGENIC Endo-Ice (COLTENE, item H05032), which contains tetrafluoroethane as the propellant, was applied to a No. 2 cotton pellet from approximately 2 cm until it was evenly saturated and frosting appeared; the spray was never directed intraorally. The manufacturer indicates that it has an Endo-Ice refrigerant system for pulp sensitivity testing and that the spray is to be applied to the "pellet" and not directly to oral tissues.

Following the 20-second LSCI baseline acquisition with the participant undisturbed in the imaging position, the refrigerated pellet was placed on the standardized mid-buccal coronal test site for exactly 5.0 seconds using light contact without enough pressure to displace the tooth or bite index. At the end of the timed exposure, the pellet was removed and the time of removal was considered as post-challenge time zero. The next 180 s recovery recording was performed without any extra thermal stimulus. The experimental cold challenge was conducted only following the prior recovery from the diagnostic sensibility testing, thus providing a stable pre-challenge speckle signal, not one that was thermally reactive from the prior challenge.

Transillumination Laser Speckle Contrast Imaging System and Optical Configuration

The imaging system used in the experiments was based on coherent near-infrared transillumination instead of surface epi-illumination. The coherent source was a 785-nm, 6.5-mW polarization-maintaining fiber-pigtailed laser diode (Thorlabs LPS-PM785-FC, nominal optical output), with FC/PC termination. The fibre output was collimated using an F220FC-780 fixed-focus collimator (Thorlabs; alignment wavelength 780 nm, focal length 11.07 mm, numerical aperture 0.26, nominal collimated beam diameter 2.1 mm). The source was set against the lingual aspect of the crown and directed through the tooth towards the buccal imaging surface. The LPS-PM785-FC is a 785-nm, 6.5-mW, single-transverse-mode PM-fiber-pigtailed laser diode as specified by the manufacturer, and the F220FC-780 is specified for 780-nm alignment with a 650–1050-nm antireflection coating.

The incident optical power at the tooth was adjusted to approximately 5.0 mW and was checked at 785 nm using a calibrated optical power meter system comprised of an optical power meter console (Thorlabs PM400 touch screen console) and a silicon photodiode sensor (Thorlabs S120C, which has a spectral range of 400–1100 nm and a measurement range between 50 nW and 50 mW).

A monochrome Basler ace U acA1920-155um USB 3.0 camera (Basler AG, order no. 106879) with a Sony IMX174 global-shutter CMOS sensor was used to record the transmitted speckle patterns. Using the camera, a default resolution of 1920 × 1200 pixels, 5.86 × 5.86-µm pixels, and a maximum manufacturer-specified acquisition rate of 164 frames/s was obtained. A 50-mm C-mount machine-vision lens (Thorlabs MVL50M23, 50-mm effective focal length, maximum aperture f/2.8) was attached to the camera, with an FBH05800-40 hard-coated near-infrared bandpass filter (Thorlabs; 12.5 mm diameter, 800 nm center wavelength, 40 nm FWHM) placed in the detection path to remove broadband room illumination while passing the 785-nm speckle signal.

Lens aperture was fixed at f/8 and focus, gain, exposure, source power, and camera geometry were never adjusted once the initial calibration was performed and within an individual participant sequence. The choice of transillumination was based on the results of the earlier model dental laser-speckle experiments that showed significantly improved discrimination of model pulpal flow in a transmission geometry compared to epi-illumination.

Patient Positioning, Tooth Stabilization, and Imaging Geometry Standardization

The participants were positioned in a semi reclined dental chair with the head supported against the headrest and were asked to try to remain still and avoid swallowing during short critical acquisition intervals. An occlusal stabilization index was created for each participant using EXABITE II NDS vinyl-polysiloxane bite-registration material (GC corporation, part no. 132412). Setting time was about 45 seconds in the intraoral setting and Shore A hardness of the registration was about 87, which enabled the registration to serve as a rigid repositioning guide after polymerization.

Stable occlusal surfaces were used in the index and did not obstruct the buccal or lingual optical pathway. The camera and source were mounted on mechanically fixed articulated mounts that were separate from the participant. At a fixed working distance of 200 mm, the camera optical axis was positioned approximately perpendicular to the central buccal

crown surface. The laser collimator was placed on the appropriate lingual aspect to have the transmitted beam cross the coronal pulp projection before it reached the detector. After achieving good focus and speckle intensity, all mount adjustments for translation and rotation were locked. To help minimize variation in magnification, angle, illumination field and speckle sampling in the baseline and post-challenge sequence, the bite registration, head support, fixed working distance, and locked camera/source mounts were used in combination.

Laser Speckle Image Acquisition and Recording Sequence

The raw monochromatic data images were taken at 100 frames/s, with an exposure time of 5 ms, and using no electronic gain. An area of interest around the clinical crown and a gingival reference area was captured in a lossless format using a camera. Acquisition was initiated prior to experimental stimulation and was uninterrupted throughout a 20-s baseline, the 5-s cold application, and the entire 180-s recovery period following stimulation removal.

Cold-contact onset and stimulus removal were marked with a digital event marker that was synchronized to the acquisition clock. Each subject then provided one continuous physiologic record from 20 s before exposure to cold and 180 s following the cold exposure. Use of autofocus, autoexposure, automatic gain correction, temporal enhancement of the image by the camera or camera-based noise reduction was not allowed during recording since any such action might affect speckle statistics. The coded raw data of the participant contained camera acquisition parameters, which were kept constant throughout the entire sequence.

Physiologic and Environmental Covariate Recording

Each subject was first allowed to get used to the examination room for a minimum of 10 minutes prior to the experimental recording. The room temperature and the relative humidity were recorded using a testo 608-H1 thermohygrometer (Testo SE & Co. KGaA, order no. 0560 6081) with a temperature range from 0–50°C and an accuracy of ±0.5°C at 25°C, and a relative-humidity range from 10–95%, with a stated accuracy of ±3% RH.

Peripheral pulse rate was measured with Onyx Vantage 9590 finger-pulse oximeter (Nonin Medical, model 9590) which has a range of 18–321 beats/min and a declared accuracy of pulse rate of ±3 digits when there are no motion effects and pulse rate is between 20–250 beats/min. Pulse rate was recorded at the resting baseline and in recovery to track large systemic hemodynamic changes that might affect the speckle signal recorded locally.

Local gingival temperature was assessed with a fine type-K thermocouple (OMEGA 5SRTC-TT-K-36-36) placed next to the optical tooth ROI, but not inside the ROI, and attached to an HH806AU dual-input temperature data logger. The thermocouple was placed against attached gingiva, but not over the field of imaging. The 5SRTC-TT-K-36-36 was a 36-inch type-K surface thermocouple and the HH806AU was a type-K thermocouple that was used to take measurements between −200 and 1372°C and storing serial temperature readings.

Quality-control and possible covariate information from environmental and systemic variables were not used to create the definition of the primary index.

Speckle Image Preprocessing and Artifact Management

Images were processed raw with coded participant identifiers, but without access to the reference diagnosis. A dark-frame image was taken with the optical path obscured and these images were subtracted from each raw image to eliminate fixed sensor offset. In all other cases, the speckle images were not denoised spatially or temporally prior to contrast computation since spatial and temporal denoising prior to contrast computation could artificially reduce the intensity variance from which the speckle signal was derived.

Rigid intensity-based registration against a baseline image of the crown was used to correct for small inter-frame translations. Registration was done prior to participant level time courses extraction, but only translation and minor in plane rotation were allowed. Frames that were not usable because of gross movement, loss of focus, transient obstruction, detector saturation or the cold pellet being displaced into the analysis region were identified in an automated quality-control pass and were checked using the coded sequence. All artifact labels and decisions regarding frame removal were made prior to the final diagnostic labels.

Tooth and Gingival Region-of-Interest Segmentation

Analysis masks were derived from a mean image created from the stable baseline sequence. The location of the principal tooth ROI was based on the crown's anatomy and the radiographically determined location of the pulp chamber prior to treatment. The mask was at least 1 mm from the visible enamel borders and excluded carious cavitation, highly reflective restorations, direct laser entry artifacts and areas prone to movement.

A gingival control ROI was drawn separately over adjacent attached gingiva that did not overlap the tooth, periodontal sulcus or cold-contact area. The gingival mask was employed to detect synchronous extra coronal perfusion signals, or motion signals that might imitate a pulpal signal. Both masks were propagated through the registered sequence (without frame-by-frame redrawing) once they were defined on the baseline reference image. This enabled the post-challenge response to be unknown to those making ROI placement.

Calculation and Baseline Normalization of the Pulpal Speckle Flow Index

For each image, the speckle contrast K is computed as the ratio of the standard deviation of the pixel intensity in the 5 × 5-pixel moving window to the mean of the pixel intensity. Speckle contrast was then transformed into a relative speckle flow index (SFI) as SFI = $1/(2TK^2)$, with T being the camera's fixed exposure time (0.005 seconds). A commonly used approximation in LSCI is the inverse relationship between the squared speckle contrast and the decorrelation time for the purpose of computing a relative flow index.

For each frame, the median SFI value of the entire valid pixels contained in the tooth ROI was determined. Frame-level values were then summarized to 1-second median values, smoothing out high frequency camera noise and maintaining the physiologic level of recovery trajectory. The median value of the last 10 seconds of the pre-challenge recording was considered the baseline value for each participant. Each of the post-challenge values was divided by this baseline value to create a dimensionless normalized flow series in which 1.00 was the individual's own resting baseline. This within-tooth normalization reduced interindividual variation in enamel/dentin optical transmission, absolute signal amplitude and pulp-chamber geometry.

Extraction of Prespecified Microvascular Recovery Features

All dynamic parameters were taken from the normalized curve (0–180 s) after the challenge using a fixed algorithm. The immediate response was determined as a percent change from the baseline for the 5 s immediately after the removal of the cold stimulus. The highest absolute displacement from 1.00 (during the initial 30 s following stimulus removal) was defined as the dominant early vascular excursion and maintained as such with the original direction, either a nadir or peak after the challenge. The extent of recovery was related to the size of this early excursion. Time to 50% recovery was set as the first time after the extremum that the absolute displacement from baseline had decreased by at least 50% and remained at or beyond that recovery level for 5 consecutive seconds. Time for 90% recovery was calculated in the same way with a 90% recovery threshold. The curves that did not reach the specified recovery level at 180 seconds were right-censored at 180 seconds for the purpose of descriptive recovery-time reporting.

The recovery slope was calculated by ordinary least-squares regression of the absolute difference from baseline measured from 10 seconds to 90 seconds after the vascular disturbance, such that a more negative slope indicates a more rapid recovery from the vascular disturbance. Trapezoidal numerical integration of the recovery-curve area from 0 to 180 s was performed. Coefficients of variation were computed for baseline and for full sequence to serve as prespecified measures of physiologic and optical signal stability.

Definition of the Primary Microvascular Recovery Index

The primary microvascular recovery index was calculated prior to unblinding of the diagnostic labels as the time-averaged absolute deviation of the normalized SFI from the pre-challenge level during the entire recovery period of 180 seconds. This was found by integrating |SFI_normalized(t) − 1| over the interval [0, 180] and dividing by 180. The index was consequently nondimensional and incorporated both the severity and the duration of the cold-induced microvascular disturbance.

The absolute deviation enabled for the same individual tooth to quantify a delayed vascular normalization, whether the initial speckle-flow signal showed vasoconstrictive decrease or hyperemic increase. A value close to zero indicated little or quick recovery from baseline and larger values indicated a greater and/or more prolonged post-challenge disturbance. This index was the one prespecified LSCI variable analyzed for the primary ROC analysis.

Signal-Quality Assessment and Recording Exclusion Criteria

Prior to the diagnostic group comparison, quality rules were locked. Individual frames were deemed invalid if more than 1% of the tooth-ROI pixels were saturated, when the residual registration error was greater than 2 pixels, when the tooth ROI was materially obscured, or because of gross subject movement which did not allow for reliable identification of the mask. Linear interpolation was performed only for short invalid intervals of 0.5 seconds or less and only when the proportion of invalid post-challenge observations remained below 10%.

A complete LSCI sequence was deemed technically nonvaluable if a greater than 10% proportion of post-challenge observations were invalid, if it was not possible to keep the usable tooth ROI across the entire sequence, if the coefficient of variation of the baseline SFI was greater than 20%, or if the optical intensity remained persistently out of the predefined usable detector range despite correct positioning. Technical data were excluded from analysis and not related to clinical group or outcome. To differentiate exclusion from a lack of a vascular reaction, signal-quality variables were kept for reporting.

Conventional Cold-Test and Electric Pulp-Test Measurements

Pre-experimental LSCI and conventional sensibility measurements were taken. A clinically normal comparison tooth was used to perform the diagnostic cold test wherever possible. An Endo-Ice No. 2 cotton pellet, prepared in the same way, was refrigerated and placed on the middle third of the buccal crown with no gingiva touching the preparation. The participants noted the first time when they could feel cold and when the coldness was gone. The time between pellet removal and the total absence of the sensation was recorded with 0.1-second resolution and defined as the conventional cold-pain-duration variable.

The Digitest 3 Pulp Vitality Tester (Parkell, SKU D655) was used for electric pulp testing. The tooth surface was isolated, the probe tip was coated with the conducting medium, and the probe was positioned on the middle third of the buccal crown surface without gingiva and metallic restorations. The slow stimulus-increase setting was employed, and participants were asked to signal when they first perceived a tingling or warm sensation. The Digitest 3 displays the stimulus levels on a 0–64 scale. Three measurements were taken, each about 2 minutes apart, and the median measurement used as the electric-pulp-test threshold. The D655 system comes with long, short, labial and lingual autoclavable probes, a lead wire, clip and 9-V battery.

Cold-response duration and electric-pulp-test threshold were kept as traditional comparator variables, and neither was used as a replacement for the composite final reference diagnosis.

Definitive Treatment Procedures and Intraoperative Findings

Definitive dental treatment was only commenced once all research imaging was completed. Treatment choice was determined by clinical status of the tooth and treatment plan was decided without regard to the LSCI results. Teeth with reversible pulpitis as provisional diagnosis, caries management was performed aiming at pulp vitality preservation. If a pulp-preserving hydraulic calcium-silicate material was clinically indicated, Biodentine (Septodont, catalog no. 01C0600; 15-capsule presentation) was used as per manufacturer's instructions. Biodentine 01C0600 is now a registered bioactive dentin substitute.

Teeth with symptomatic irreversible pulpitis were either treated with the clinically indicated vital-pulp procedure or conventional root-canal treatment. The operator rendered a note concerning the exposure of the pulp, whether vital bleeding was encountered, the macroscopic character of the tissue, the presence of focal nonbleeding or necrotic tissue and the ability to obtain clinically acceptable hemostasis when a vital-pulp procedure was performed. No surgery was prolonged, nor was pulp tissue removed simply for the purposes of a research specimen. These findings were made prior to the final adjudication per the reference standard, and without the use of the LSCI-derived index.

Pulp Tissue Collection and Histopathologic Processing

Only those symptomatic-irreversible-pulpitis teeth where removal of the coronal pulp tissue was already a part of the planned pulpotomy or root-canal procedure had pulp tissue collected. Tissue was obtained prior to the placement of pulpal medicaments and was immediately placed in 10% neutral buffered formalin (Sigma-Aldrich/MilliporeSigma, catalog no. HT501128) that contained formaldehyde at approximately 4% and a pH of 6.90–7.10. The volume of fixative to tissue was at least 10:1 and the tissues were fixed at room temperature for about 24 hours.

After fixation, the specimens were dehydrated in graded alcohols, cleared, paraffin imbedded, and cut into 4-µm sections. Multiple levels were examined to decrease the likelihood that a small focus of inflammation or necrosis would be missed, and they were not adjacent. Hematoxylin and eosin staining was performed by using Abcam H&E Staining Kit (ab245880). Using the kit protocol, sections were deparaffinized, hydrated and stained for 5 minutes with modified Mayer hematoxylin, 10–15 seconds with bluing reagent and 2–3 minutes with modified alcoholic eosin Y before dehydration, clearing and mounting.

Histologic slides were coded only with the study code and were evaluated without knowledge of the laser-speckle results.

Histopathologic Inflammation and Tissue-Injury Scoring

Histologic evaluation was based on the features a priori selected as signs of inflammatory severity of the pulp. The inflammatory-cell infiltrate was rated in the most affected viable area as absent/minimal, mild, moderate, or severe. In terms of quantity, grades 1, 2 and 3 corresponded approximately to fewer than 30, 30–60, and more than 60 inflammatory cells, respectively, within the representative high-power field, while grade 0 indicated absence of a meaningful inflammatory infiltrate. The predominant inflammatory pattern and the presence of polymorphonuclear leukocyte accumulation were also recorded.

Vascular congestion was also scored based on the number and distribution of clearly dilated and congested vascular profiles in the most involved field. Tissue necrosis was documented

as none or present, and if present as either focal or more widespread. Microabscess was defined histologically as a localized accumulation of neutrophilic inflammatory cells associated with tissue breakdown and was reported separately as absent or present. These features demonstrated the well-known development of localized inflammatory change to polymorphonuclear infiltration, microabscess formation, and partial necrosis of the pulp tissue as described histologically in advanced pulpitis.

An overall histopathologic severity grade (0–3) was used for correlation analysis. Grade 0 was essentially preserved architecture with no or very low grade of inflammation, grade 1 was mild localized inflammation without necrosis or formation of microabscess, grade 2 was moderate inflammatory involvement and/or marked vascular congestion without destructive necrosis, and grade 3 was severe inflammatory infiltration, definite pulp-tissue necrosis, or the presence of microabscesses. The global grade was fixed prior to correlating with the LSCI variables.

Six-Month Clinical and Vitality Follow-Up of Reversible Pulpitis Cases

Reversible-pulpitis group participants were called back about 6 months after treatment. Follow-up involved a structured history regarding spontaneous pain, cold sensitivity, night symptoms, difficulty chewing, unscheduled dental visits, pain medication use for the treated tooth and any intervening endodontic treatment. Restoration integrity, swelling, sinus tract formation, palpation tenderness, percussion tenderness and clinically relevant mobility of the tooth were assessed.

These tests were repeated at the next visit using the same clinical testing principles as at baseline but were performed as a cold sensibility test and an electric pulp test. Periapical radiographs were then analyzed for new periodontal-ligament widening, loss of lamina dura or developing periapical radiolucency on a follow-up periapical radiograph. A tooth with a good vitality-compatible sensibility response and no new apical pathosis, but persistent clinically functional, symptom-free tooth, confirmed the original reversible-pulpitis diagnosis. Spontaneous pulpal pain, insensitivity with clinical evidence of necrosis, new apical disease and the need for endodontic intervention was considered evidence against sustained reversible disease and were referred to the adjudication committee.

Composite Reference-Standard Adjudication

Notably, the final reference classification was determined without regard for the LSCI result after all the clinically available reference information was matured. The pain phenotype of pre-treatment, conventional examination findings, definitive treatment observations, histopathology (if tissue was extracted as part of definitive treatment) and 6-month clinical course of teeth treated as reversible pulpitis were all part of the adjudication process.

Strong reference support was defined as a typical symptomatic phenotype and intraoperative findings of a vital inflamed pulp and, if available, histologic evidence of significant inflammation, vascular damage, microabscess, or necrosis for symptomatic irreversible pulpitis. The best reference evidence for reversible pulpitis was symptom resolution with maintenance of pulp sensibility/vitality and no new apical disease on follow-up. Histology was not required from conservatively managed reversible cases because obtaining tissue would itself have violated the intended pulp-preserving treatment strategy.

The laser-speckle maps, normalized recovery curves, primary recovery index or any derived feature of LSCI were not provided to adjudicators. This final binary referent label was finalized prior to diagnostic-accuracy analysis. This composite standard was used because no single clinical sensibility test could provide a direct histologic gold standard for all vital teeth, and by taking destructive tissue samples from the reversible group, there would have been a clinical and ethical problem.

Examiner, Operator, Pathologist, and Analyst Blinding

Various research functions were dissociated to reduce bias in the review and incorporation of the studies. The examiner acquiring the laser-speckle recording was not told what the final adjudicated reference diagnosis was. The LSCI maps, recovery curve, recovery index and preliminary diagnostic interpretation that were created from the imaging sequence were not available to the clinician performing definitive treatment.

Histologic specimens were coded prior to their delivery to the pathologist who was blinded to the results of the LSCI. Imaging files were coded with noninformative participant codes prior to the preprocessing and ROI extraction, and the main imaging analyst was blinded at the time of preprocessing to the final diagnostic group. The second analyst for reproducibility assessment was independent, and only coded raw image sequences were handed to him. LSCI-derived diagnostic classification was also held in blind form during the adjudication process by members of the reference-standard adjudication process until the reference labels were finalized.

Inter-Analyst Reprocessing and Reproducibility Assessment

A 20% sample of the recordings (10 recordings) were randomly selected using computer-generated random sampling and independently re-segmented by a second analyst who was not involved in original segmentation. The second analyst repeated the process of registration, ROI definition (teeth and gingival), extraction, normalization, and calculation of the primary microvascular recovery index, using the locked processing instructions.

A two-way random-effects, absolute-agreement, single-measure intraclass correlation coefficient ICC (2,1) with a 95% confidence interval was used to quantify the agreement for the continuous primary recovery index. A Bland–Altman analysis was also performed to calculate the mean difference and 95% limits of agreement between the analysts. Short-term baseline signal stability was tested by comparing SFI estimates from the first and second 10-s baseline intervals within each recording as well as by using the baseline coefficient of variation. Reproducibility analyses were carried out separately from the main diagnostic comparison.

Study Outcomes and Endpoint Definitions

The ROC area under the curve of the prespecified microvascular recovery index was the primary study endpoint for distinguishing symptomatic irreversible pulpitis from reversible pulpitis according to the locked composite reference standard.

Secondary endpoints included the between-group difference in the immediate vascular response, extremum, time to 50% recovery, time to 90% recovery, 10–90-second recovery slope, 0–180-second recovery-curve area, the increase in diagnostic information provided by LSCI when used in combination with cold-response duration and electric-pulp-test threshold, inter-analyst agreement, baseline signal reproducibility, and 6-month symptom and vitality status for the reversible-pulpitis group.

The prespecified diagnostic biomarker was the microvascular recovery index. All other dynamic characteristics were kept as secondary or auxiliary measurements to avoid a post hoc selection of the best part of the recovery curve.

Sample Size and Statistical Power Calculation

The evaluable sample size was determined to be 50 participants, 25 participants for the reversible-pulpitis group and 25 participants for the symptomatic-irreversible-pulpitis group. This sample was able to detect a standardized between-group difference of 0.81 on the continuous primary recovery measure with approximately 80% power at a two-sided type-I error rate of 0.05 with equal group allocation and 25 observations per group.

The calculation of power was based on the participant-level recovery index, not the number of LSCI frames. Multiple frames of images were used to boost temporal resolution of each participant's physiologic curve, but not the nominal sample size. No single video frame was considered as an independent observation in the

power calculations or the diagnostic-accuracy analysis, and no more than 50 evaluable participants were included in the final analysis.

Statistical Analysis

The current stable release of R (version 4.6.1, R Foundation for Statistical Computing, Vienna, Austria) was used for all statistical analyses. The continuous variables with approximately normal distribution were summarized as mean ± standard deviation and compared between the RP group and the SIP group using two-sided Welch independent-samples t test. Cold-response duration and T90 were summarized as the median and interquartile range and compared using the two-sided Mann–Whitney U test; T90 was summarized nonparametrically as a measure being bounded at 180 s. Categorical variables were presented as frequencies and percentages and compared by two-sided Fisher exact test. Effect size between groups was reported using Hedges' g for continuous normally distributed variables, odds ratio for categorical variables, and rank-biserial correlation for variables evaluated using Mann–Whitney U test, along with associated 95% confidence intervals where possible. A maximum-likelihood linear mixed-effects model with participant-specific random intercepts and fixed effects for time, diagnosis and the diagnosis-by-time interaction was used to analyze a full 180-s recovery trajectory of normalized LSCI. A flexible model for time was used, namely a natural cubic spline with four degrees of freedom. Wald χ^2 tests were used to test for global fixed effects and contrasts between RP and SIP at chosen recovery times were obtained from the fitted fixed-effect covariance matrix. Marginal and conditional R^2, Akaike information criterion, and Bayesian information criterion were used to characterize model performance. The LSCI recovery index, cold-response duration and EPT threshold were assessed for their diagnostic accuracy at the participant level using receiver operating characteristic analysis. AUCs were reported with 95% confidence intervals derived by 10,000 stratified bootstrap resamples. DeLong covariance estimates were used to assess the statistical significance of each AUC compared to 0.50 and also for the pairwise comparison between correlated ROC curves. Operating cutoffs for each diagnostic measure were chosen to maximize Youden J statistic. Sensitivity and specificity were reported with Wilson 95% confidence intervals, positive and negative likelihood-ratio confidence intervals were calculated on the logarithmic scale; the higher the test value, the more indicative of SIP. For Figure 1, incremental diagnostic performance was assessed with binary logistic regression. The conventional model contained cold-response duration and EPT threshold, whereas the extended model also included the prespecified LSCI microvascular recovery index. AUCs for paired predictions from the same participants were compared using the paired DeLong procedure, improvement in nested model fit was assessed using the likelihood-ratio test, and the independent contribution of the LSCI index was evaluated from its regression coefficient and associated p value. For Figure 2, Spearman rank correlation (Spearman's ρ and p value) was used to assess the correlation between LSCI recovery index and ordinal histopathologic severity in SIP cases in which tissue was available. The two-way random-effects, absolute-agreement, single-measure intraclass correlation coefficient (ICC(2,1)) was used to quantify inter-analyst reproducibility of LSCI processing, and the 6-month confirmation of RP cases was reported descriptively as a frequency and percentage. Figures 3–7 represent the representative native imaging, radiographic, and histopathologic illustrations and were not individually inferentially statistically tested; the quantitative data mentioned in their captions were based on the related analyses described above. All statistical tests were two-sided, statistical significance was set at $p<0.05$, and no multiplicity adjustment was made in the secondary comparisons of the LSCI recovery variables.

Ethical Approval and Informed Consent

The study protocol was approved by the institutional research-ethics committee prior to enrollment of participants, and all procedures were carried out in accordance with ethical principles for research with human subjects. All participants provided written informed consent prior to imaging or research data collection as part of the study. The process of participating in the imaging study did not result in or delay in any necessary dental treatment and no pulp tissue was removed just for the purposes of the imaging study.

For all participant data and imaging files, coding was performed prior to analysis and study codes and personal identifiers were kept in a separate file. The study was carried out according to the Declaration of Helsinki of the World Medical Association, including the 2024 revision on medical research involving human subjects.

The laser operation was based on IEC 60825-1 laser-product safety. Inadvertent direct viewing of the source was avoided, and wavelength appropriate protective measures were implemented by the operator and participant when the exposed beam was accessible; the 785-nm beam was only used during positioning checks and image acquisition.

Results

Approximately normally distributed continuous variables were compared using Welch's independent-samples t test and are reported as mean ± SD. Cold-response duration was analyzed using the two-sided Mann–Whitney U test and is reported as median [IQR]. Categorical variables were compared using two-sided Fisher's exact test. Effect sizes are Hedges' g, odds ratios (OR), or rank-biserial correlations, as appropriate. All tests were two-sided, and $p<0.05$ was considered statistically significant.

The groups were well balanced for age, sex, dental arch, molar type, and radiographic caries-to-pulp distance, with no statistically significant baseline structural differences. In contrast, the SIP group demonstrated a distinctly more severe symptomatic phenotype. Spontaneous pain, nocturnal pain, lingering thermal pain, and percussion sensitivity were significantly more frequent in SIP, with particularly large odds ratios for spontaneous and lingering pain. Cold-response duration was substantially prolonged in SIP, with a large rank-biserial effect and strong statistical significance. Electric pulp-testing thresholds showed only modest numerical elevation in SIP and did not differ significantly between groups, supporting their relatively limited discriminative value.

Patient-level approximately normally distributed LSCI variables were compared using Welch's t test. T90 was analyzed using the two-sided Mann–Whitney U test because recovery time was bounded at 180 s. Hedges' g and rank-biserial correlation quantify effect magnitude. A more negative 10–90 s recovery slope represents a faster reduction of absolute deviation toward baseline. Two-sided $p<0.05$ was considered significant. Secondary comparisons were not adjusted for multiplicity.

Technical recording quality was comparable between groups, as neither baseline signal variability nor rejected-frame percentage differed significantly. SIP produced a greater immediate vascular disturbance after cold challenge, whereas the difference in maximum early excursion did not independently reach significance. The major differences emerged during recovery. The prespecified recovery index was more than twice as high in SIP and showed a very large, standardized effect. Both T50 and T90 were substantially prolonged, demonstrating markedly delayed normalization of pulpal microvascular flow. RP also exhibited a significantly steeper negative recovery slope, indicating faster restoration toward baseline. Consequently, integrated absolute recovery-curve area was approximately doubled in SIP.

A maximum-likelihood linear mixed-effects model included participant-specific random intercepts and fixed effects for diagnostic group, time, and diagnosis×time. Time was modeled using a four-degree-of-freedom natural cubic spline. Global fixed effects were assessed using Wald χ^2 tests. Selected-time contrasts were

obtained from the fitted fixed-effect covariance matrix. Time 0 represented the immediate post-challenge recovery point rather than the pre-challenge normalized baseline. Two-sided $p<0.05$ was considered significant.

Mixed-effects modeling demonstrated a pronounced difference in the temporal recovery pattern between RP and SIP. The diagnosis-by-time interaction was exceptionally strong, confirming that group separation depended on recovery time rather than representing only a constant difference in normalized flow. SIP showed lower normalized SFI throughout most of the early and intermediate recovery period. The largest modeled separation occurred around 60 seconds, when the SIP value remained approximately 0.084 below RP. Significant differences persisted through 120 seconds, whereas the groups had effectively reconverged by 180 seconds. The high marginal and conditional R^2 values indicated that the fitted longitudinal model explained most of the recovery variability.

AUCs were calculated at the participant level. Their 95% CIs were estimated using 10,000 stratified bootstrap resamples. Significance of each AUC relative to 0.50 and comparisons between correlated ROC curves were evaluated using DeLong covariance estimates. Diagnostic cutoffs maximized Youden J. Sensitivity and specificity CIs were calculated using Wilson intervals, and likelihood-ratio CIs were calculated on the logarithmic scale. Higher values indicated SIP. All tests were two-sided, with $p<0.05$ indicating statistical significance.

The prespecified LSCI recovery index demonstrated excellent discrimination between RP and SIP, achieving an AUC of 0.9088. Its principal strength was high specificity, reaching 96%, with a positive likelihood ratio of 18. Cold-response duration also performed well and provided somewhat higher sensitivity, although its AUC was numerically lower at 0.8528. The 0.056 AUC advantage of LSCI over cold testing did not reach statistical significance in this 50-participant sample. In contrast, LSCI significantly outperformed EPT by an AUC difference of 0.3032. EPT alone was not significantly superior to chance and showed limited diagnostic utility.

Among the 22 symptomatic irreversible pulpitis cases with available pulp histology, increasing histopathologic severity was associated with progressively greater disturbance of post-cold microvascular recovery. The LSCI recovery index showed a significant positive correlation with the ordinal histopathologic severity grade (Spearman ρ=0.551, p=0.00788), indicating that more severe inflammatory and tissue-destructive changes tended to accompany larger and more persistent vascular abnormalities. The dataset additionally demonstrated excellent inter-analyst reproducibility for LSCI processing, with ICC (2,1)=0.993. Among reversible-pulpitis cases, 23 of 25 teeth (92%) maintained successful six-month reference-standard confirmation, supporting the stability of the conservative diagnostic classification.

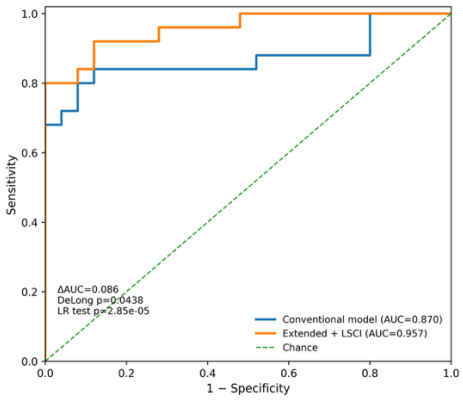


Figure 1. Incremental diagnostic performance of the LSCI recovery index beyond conventional pulp sensibility tests.

The conventional model incorporating cold-response duration and EPT threshold demonstrated good discrimination between reversible and symptomatic irreversible pulpitis, with an AUC of 0.8704. Addition of the LSCI microvascular recovery index increased the AUC to 0.9568, corresponding to an absolute improvement of 0.0864. The paired DeLong comparison indicated that this improvement was statistically significant (p=0.0438). Model fit also improved substantially, with the likelihood-ratio test favoring the extended model (χ^2=17.516, p=0.0000285). Importantly, the LSCI recovery index remained independently associated with symptomatic irreversible pulpitis after adjustment for both conventional sensibility measures (p=0.0111), supporting its incremental physiologic diagnostic contribution.

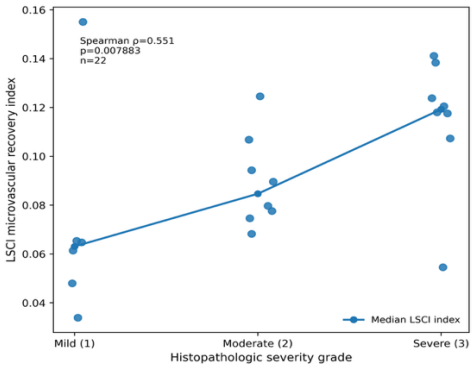


Figure 2. Association between histopathologic severity and the LSCI microvascular recovery index in symptomatic irreversible pulpitis.

Among the 22 symptomatic irreversible pulpitis cases with available pulp histology, increasing histopathologic severity was associated with progressively greater disturbance of post-cold microvascular recovery. The LSCI recovery index showed a significant positive correlation with the ordinal histopathologic severity grade (Spearman ρ=0.551, p=0.00788), indicating that more severe inflammatory and tissue-destructive changes tended to accompany larger and more persistent vascular abnormalities. The dataset additionally demonstrated excellent inter-analyst reproducibility for LSCI processing, with ICC (2,1)=0.993. Among reversible-pulpitis cases, 23 of 25 teeth (92%) maintained successful six-month reference-standard confirmation, supporting the stability of the conservative diagnostic classification.

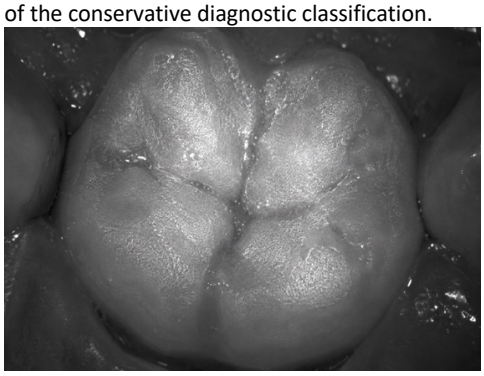


Figure 3. Native baseline near-infrared transillumination Laser-speckle frame of a representative pulpitis tooth.

This native baseline speckle frame documents the optical signal quality before thermal provocation and demonstrates a stable interference pattern suitable for quantitative LSCI processing. The recording contains minimal motion, adequate exposure, and no detector saturation. In the dataset, baseline SFI variability remained comparable between reversible pulpitis and symptomatic irreversible pulpitis, averaging 5.07% and 5.48%, respectively, with no significant difference (p=0.1888). The baseline image therefore documents acquisition quality rather than disease separation. It supports the reliability of subsequent within-tooth normalization and confirms that later differences in recovery arose after cold challenge rather than from major baseline optical instability.

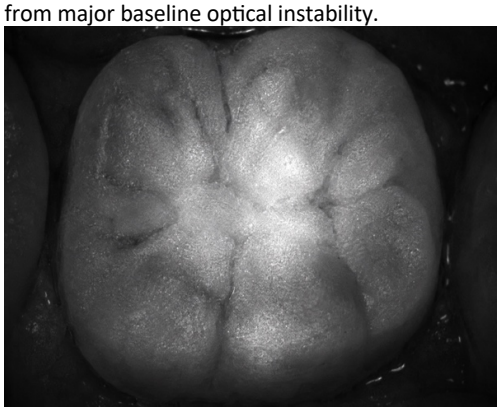


Figure 4. Native post-cold Laser-speckle frame during delayed microvascular recovery in symptomatic irreversible pulpitis.

This native post-cold frame represents the period of maximal separation between the two diagnostic groups. In the mixed-effects analysis, symptomatic irreversible pulpitis remained substantially displaced from normalized baseline around 60 seconds, with an estimated normalized SFI of approximately 0.873 compared with 0.956 in reversible pulpitis. The SIP group also demonstrated a larger primary recovery index, prolonged T50 and T90, and a greater integrated absolute recovery-curve area. The raw frame itself remains visually subtle because LSCI discrimination depends on speckle-contrast statistics rather than obvious gross brightness changes. The image documents the direct optical source signal underlying the delayed microvascular recovery phenotype.

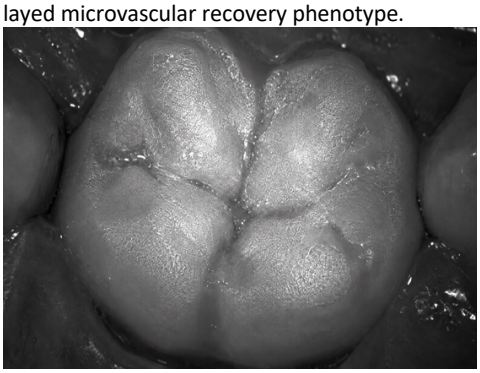


Figure 5. Native Laser-speckle frame demonstrating near-baseline recovery in reversible pulpitis.

This native late-recovery frame documents rapid restoration of the pulpal microvascular signal in reversible pulpitis after cold challenge. In the analysis, normalized SFI approached 0.99 by 90 seconds and approximately 0.999 by 120 seconds, whereas symptomatic irreversible pulpitis remained lower at approximately 0.92 and 0.958, respectively. Reversible pulpitis also demonstrated shorter T50 and T90 and a significantly steeper recovery slope. The raw image retains a realistic monochrome speckle appearance because recovery is quantified from the speckle statistics rather than from visible color or brightness changes. The frame directly illustrates the stable optical source signal corresponding to near-complete physiologic recovery.



Figure 6. Native digital periapical radiograph of an eligible mature molar with deep caries and preserved apical structures.

This native periapical radiograph documents the structural eligibility of the enrolled molars and confirms that the diagnostic comparison involved mature vital teeth with deep caries rather than necrotic, previously treated, or structurally excluded cases. In the baseline analysis, the two groups showed no significant imbalance in arch distribution, first-versus-second molar distribution, or radiographic caries-to-pulp distance. Mean caries-to-pulp distances were approximately 0.61 mm in reversible pulpitis and 0.52 mm in symptomatic irreversible pulpitis. The radiograph therefore serves as an anatomical eligibility image and supports the validity of the planned vital-pulp comparison rather than acting as a direct discriminator between the two diagnoses.

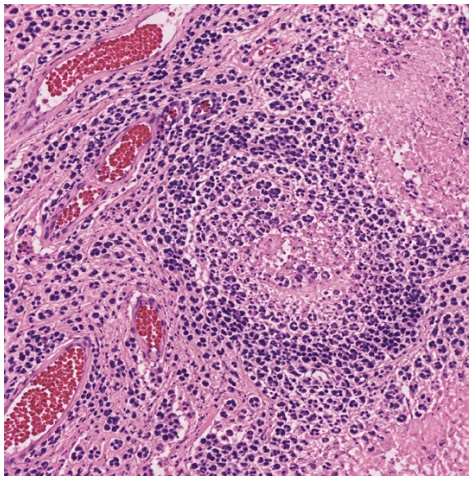


Figure 7. Native H&E photomicrograph of severe symptomatic irreversible pulpitis showing neutrophilic inflammation, vascular congestion, microabscess formation, and focal necrosis.

This photomicrograph is used for morphologic validation of the physiologic abnormalities detected by LSCI in the symptomatic irreversible pulpitis. For the histologic data set, there was a significant correlation between the LSCI microvascular recovery index and increasing histopathologic severity (Spearman ρ=0.551, p=0.0079). Larger and more persistent microvascular disturbances after cold were thus accompanied by severe inflammatory infiltration, vascular congestion, neutrophil rich inflammation, microabscess formation and focal necrosis. Histologic picture is direct evidence of the advanced pulpal injury and biological context for the delayed recovery phenotype. Histology is still limited to the SIP cases with tissue yield as the teeth with reversible pulpitis were managed without tissue extraction.

Discussion

Results from Table 2 show that the separation between reversible pulpitis (RP) and symptomatic irreversible pulpitis (SIP) could not be due to unequal quality of optical recording. There were no differences in baseline SFI variability or rejected-frame percentages between groups, and the principal separation occurred after the cold challenge, specifically during recovery. The primary microvascular recovery index was 0.0444 ± 0.019 in RP and 0.094 ± 0.0325 in SIP, with a very large, standardized effect (g = 1.834). T50 almost doubled from 36.9 to 69.8 seconds, median T90 increased from 72 to 132 seconds, and the integrated absolute recovery area approximately doubled. The clinical implications of these results are that the magnitude of the initial microvascular response to cold exposure is not as important as the persistence of that disturbance as the discriminatory signal. This is consistent with the findings by Xiong and collaborators who showed that SFI varied markedly with flow rate in an ex vivo flow model of dental pulp and had a positive correlation to flow velocity in the model, and thickness of dentin affected the SFI measured in the model. Their observations lend physical support to SFI as a flow-sensitive parameter although the model of the single isolated tooth they used did not simulate the inflammatory response, neural control or living pulp constricting circulation in response to pressure. The present study goes beyond this technical finding and demonstrates that temporally normalized SFI can provide clinically meaningful disease information in vivo [15].

The results of Table 2 are also in agreement with those derived from another objective method of measuring microcirculatory volume. Nemeth et al. used laser Doppler flowmetry to quantify dental-pulp flow and discovered significantly lower flux values in teeth with advanced caries as compared to those with minimal caries and in active versus inactive caries. Importantly, however, there was only fair agreement between vascular measurement and conventional cold or electric testing with κ values of 0.232 and 0.354, respectively. The significance of this to the present study is clinically because it lends credence to the idea that neural sensibility and vascular physiology are related but not equivalent dimensions of pulpal status. The current study introduces an important temporal dimension: The dominant excursion of early vascular activity did not differ significantly between RP and SIP ($p = 0.077$); however, the recovery index (T50, T90, recovery slope and cumulative disturbance) were much more clearly separated. So, it is possible that a pulp can react to the cold treatments in both disease conditions, but the ability to normalize the microcirculation seems more relevant than merely the ability to react [16].

Oo and co-workers have shown in 30 healthy maxillary incisors that a thermal challenge can cause reversible changes in the pulpal circulation. They showed that innocuous cooling produced a significant decrease in the circulatory signal in the pulp using transmitted-light plethysmography and that the signal recovered to near baseline following the removal of the stimulus. They also did not discover a significant serial correlation between the changes recorded and autonomic activity, implying that a significant local component is present to the response. The present study agrees with this physiology but shows that the recovery phase can become diagnostically informative when diseased teeth are compared to other teeth. The relative rapid normalization in RP would seem to be a preserved homeostatic response, while the significantly longer T50 and T90 in SIP would be a reasonable interpretation of reduced micro vascular resilience after provocation. Although they are not directly comparable, Oo and colleagues studied healthy incisors with a significantly different cooling protocol and a different optical method, but a vascular change that is reversible and time dependent was observed after cold in both studies, giving some mechanistic validity to the challenge-recovery paradigm employed in the current study [13].

Lam and colleagues contribute further evidence of the difference between blood-flow behavior and conventional sensibility responses by prospectively measuring pulp blood flow with laser Doppler flowmetry along with electric and thermal sensibility testing during rapid maxillary expansion. They demonstrated that vascular behavior can be altered with time and that prior dental trauma might affect behavior of the vessels even if clinically, sensibility remains. This observation is especially pertinent to the present study since EPT is essentially a neural response test, while LSCI recovery index is reflective of vascular dynamics. The results obtained here reflect the same sort of "vascular" dissociation: Both SIP and RP had a measurable response, but the vascular pathway of both after the challenge was dramatically different. Clinically, this can be used to help consider LSCI as not just as another way to show "vitality" but as a tool to assess the ability of a "vital" pulp to regulate perfusion following stress. Due to the difference in study populations (orthodontically treated anterior teeth and carious mature molars), it is not possible to make direct, quantitative comparisons, but the physiological principle is the same [17].

Further evidence for the importance of dynamic recovery over a single measure is provided by Yin and others. LSCI identified significant changes in gingival blood flow over time following orthodontic forces, with the heavy force group showing a greater decrease in gingival blood flow that, in turn, recovered. While the physiology of gingival perfusion over days is not the same as the physiology of pulpal microcirculation over seconds, the study also shows that LSCI is able to capture physiologically meaningful vascular trajectories and the time course of vascular recovery carries information regarding the magnitude of the tissue stress. For the current study, the absolute difference between the groups at immediate follow-up was relatively small (about 20.0% versus 23.1%), but the standardized differences at later follow-up were much higher. This trend further confirms the clinical case for using short static LSCI measurements, which may not capture diagnostically valuable data. Standardized stimulation with continuous monitoring of recovery seems more promising to detect disturbed vascular regulation than either resting flow or the early excursion to a maximum [18].

Table 3 supports the main result by showing that RP and SIP not only differed on summary variables, but also on the shape of the overall recovery curve over 180 seconds. There was a very strong diagnosis-by-time interaction, with the modeled difference changing from −0.0257 immediately after challenge to −0.0836 at 60 s, being significant at 90 and 120 s, and not at 180 s. This reconvergence has clinical significance, SIP did not function as a permanently nonperfused or necrotic pulp, but as a vital pulp with a delayed restoration of vascular homeostasis. Galler and colleagues defined dental-pulp inflammation as a complex, interacting cellular, vascular, neural, and immune phenomenon that occurs within the confines of hard mineralized structures and that inflammatory signals and vascular changes have the potential to significantly influence tissue homeostasis. Their pathophysiological theory would explain the current trend, inflammatory vasomotor disturbance and permeability and tissue pressure changes can lengthen the period of recovery without completely stopping the circulation. This also correlates with the modern understanding that pulpitis is a continuum of tissue damage and does not just have two binary options: vascular or not [19].

The grouping of the temporal data in Table 3 is biologically consistent with the molecular inflammatory differences found by Hasan et al. Their ex vivo study of irreversibly inflamed human pulps revealed high inflammatory activation in diseased pulp, as evidenced by the expression of innate immune receptors and inflammatory mediators such as TLR-related, Dectin-1, osteopontin and cytokine pathways. Their findings support their hypothesis that there are biological processes beyond sensory nerve activation that occur with clinically advanced pulpitis. The maximal RP–SIP vascular separation was observed in the present study at around 60 seconds and not immediately after cooling, indicating that vascular separation may be most noticeable during efforts to restore perfusion, rather than at the time of stimulation, due to alterations in inflammatory regulation. Clinically, this is reasonable as an inflamed pulp may be able to have an initial vascular response, but the ability of the pulp to return to equilibrium in terms of vascular tone, intrapulpal pressure and blood flow may be reduced. Thus, the current LSCI trend can be viewed as a biological manifestation of an inflammatory microenvironment different in function, without LSCI itself identifying any molecule [20].

Wang et al. complemented with molecular data, in which they identified 166 immune-related genes that are differentially expressed in pulpitis and enrichment of pathways such as chemokine signaling, TNF signaling and NF-κB signaling. They stress that pulpitis is not just a general inflammatory process but the orchestration of recruitment and signaling of immune cells. This heterogeneity may contribute to the apparent partial overlap of individual RP and SIP measurements in the current study and the very strong group-by-time effect. The clinical diagnosis is a composite of multiple cellular and vascular events: varying inflammatory signaling pathways can result in varying levels of microvascular dysfunction. Hence the high marginal and conditional R^2 values indicated in Table 3 should not be taken as a sign that all diseased pulps have the same vascular pattern.

Rather, the overall trajectory, within a clinically informative time window (30–120 seconds), carries a probabilistic physiological signature, with individual biological variability. This is in line with the current molecular data on the heterogeneous inflammatory regulation of pulpitis [21].

Wang and colleagues shed further light on the mechanism that could account for the slow recovery path by studying the different types of cell death (apoptosis, pyroptosis, necroptosis and NETosis) within the different histologically defined stages of pulpitis. They showed differential expression of regulated cell-death pathways as a function of tissue status, with increased expression of necrotic-cell burden and neutrophil/NET-associated changes in pulpitis with necrosis. These findings support the view that pulp inflammation affects the pulp tissue qualitatively, rather than quantitatively, as it advances. The results of the current study also suggest that the amplitude of the initial flow change is not a sufficient representation of a SIP; the most prominent abnormality associated with a SIP is the persistence of the disturbance. From a clinical perspective, a prolonged recovery period may thus be the functional outcome of a progressive inflammatory microenvironment featuring vascular congestion, neutrophilic inflammation and local tissue damage. However, the eventual return of both groups to around 1.0 at 180 seconds is significant as it suggests that there was no complete necrosis in the teeth used in the study and that the delayed recovery was not equal to complete necrosis [22].

These very strong Table 3 separations should be viewed, however, considering the known continuum of pulpal pathology associated with caries. In a histological study of 68 untreated cavitated permanent teeth, Demant and colleagues found that extremely deep carious lesions were significantly more likely to demonstrate bacteria in contact with pulpal tissue and inflammatory infiltration and partial necrosis, while radiographically deep lesions more likely showed bacteria penetrating only primary dentin. Their results corroborate the biological pathway of the current study that shows that there is a progressive disruption of the pulp environment as disease severity increases. Their results, however, depended on the depth of the lesion and its histology rather than RP/SIP labels and they pointed out that tissue pathology is spatially heterogeneous and not necessarily a perfect fit for a binary clinical label. This is a helpful qualification of the highly significant p values reported in Table 3. The statistical significance can be very large with densely sampled longitudinal observations and, clinically, more emphasis should be placed on the magnitude of separation (30–120 s), its duration and on its validation in other cohorts [23].

Table 4 shows clinically important diagnostic performance of the prespecified LSCI recovery index. Its AUC was 0.9088, and at the cutoff of 0.0709 it achieved 72% sensitivity, 96% specificity and an LR+ of 18.0. Cold-response duration was also well discriminated (AUC 0.8528), with a higher sensitivity of 84%, but lower specificity of 88%, as EPT only produced limited discrimination (AUC 0.6056). There was no significant difference between the LSCI and the cold AUC, but LSCI was significantly greater than EPT. Similarly, Patro and colleagues found in their systematic review and meta-analysis that the pooled diagnostic odds ratios for pulse oximetry, EPT, cold testing and heat testing were 628.5, 10.75, 17.24 and 3.47, respectively, and that vascular pulse oximetry had higher pooled sensitivity and specificity than EPT or thermal testing methods. Their study examined vitality, instead of discrimination of two inflammatory states that are vital, but it confirms that direct vascular information may include diagnostic information not provided by neural sensibility alone [11].

In permanent immature teeth, Molaasadolah et al. also observed that pulse oximetry was more accurate than cold testing or EPT. Depending on the type of tooth and the degree of root development, the accuracy for pulse-oximetry reached around 98.7%–100%, while EPT and cold testing were approximately 76.2%–92.5% and 85%–92.5% accurate, respectively. These findings are like the present study and suggest that vascularly based measurements might be superior to neural-response testing, especially EPT. But the diagnostic challenge was much simpler – to differentiate vital untreated teeth from endodontically treated negative controls – instead of RP from SIP with both pulps vital and responsive. The lower sensitivity of the current LSCI cut-off should therefore not be interpreted as evidence of less advanced technology but rather as a more subtle biological limit. Clinically, the 96% specificity and LR+ of 18 are particularly useful because a markedly abnormal recovery index could significantly help to increase confidence that a symptomatic vital pulp belongs to the SIP phenotype and a negative LSCI result alone would be less useful due to the 72% sensitivity [24].

Evidence of the potential value of objective circulation-based testing is also more recent. Gupta and colleagues investigated the results from seven studies involving 654 teeth and found the sensitivity for pulse oximetry ranged from 81% to 100% with a mean of about 95%, and specificity ranged from 94% to 100% with a mean of about 99%. Again, the difference in target condition should be emphasized, and these high values are directionally consistent with the high specificity of the current LSCI recovery index. Most vitality studies are based on the question of whether perfusion exists, while the present study is based on the question of whether there is a significant difference in the behavior of a pulp already perfused following cold stress to distinguish two inflammatory phenotypes. The AUC value for the current study, therefore, 0.9088, is good for a more challenging diagnostic task. Concurrently, it was demonstrated that the next step in development is external validation of the 0.0709 threshold with other molar dentitions, dentin thickness, and restoration configurations and clinical contexts prior to its use in clinical practice [25].

The EPT performance in the current study is somewhat at odds with all recent evidence. Zeb Jan and others evaluated and measured the diagnostic accuracy of EPT in single-rooted teeth diagnosed as irreversible pulpitis and found approximately 93.9% diagnostic accuracy of EPT compared to approximately 76.7% for cold testing and concluded that EPT was more reliable in determining the pulp vitality of the single-rooted tooth. This is in direct contrast to Table 4 where EPT yielded an AUC value of only 0.6056, and the significance revealed that EPT was significantly less than both LSCI and cold-response duration. The apparent conflict can be easily explained by the difference in the diagnostic question. Zeb Jan and colleagues explored whether pulp was vital in a sample defined as irreversible pulpitis, and the present study involved EPT to differentiate the two vital inflammatory conditions. A neural threshold may be very discriminating when it comes time to differentiate between responsive tissue and nonresponsive tissue, but it may be very poor at separating both groups of tissue where functional sensory fibers are present. Consequently, the divergent results lend support to the need to define the target condition prior to comparing values for diagnostic accuracy between different pulp tests [26].

Donnermeyer and co-authors offer a caution in interpreting the Table 4 AUC as a definitive solution to pulp diagnosis in their systematic review. In 28 of the reviewed studies, they found that there are no optimal clinical tests or clinical signs to assess the actual histology of pulp inflammation. They found that there was a trend towards the diagnostic odds ratio being more likely to be high for cold testing than for EPT and suggested that a “diagnostic package” made up of various sources of information will likely be used in the future for diagnosis. Like the present results they conclude that the duration of cold response is far more informative than EPT but also warn against the use of a new biomarker as a replacement for traditional clinical assessment. The current study lends

weight to this interpretation: LSCI achieved higher numerical AUC than cold testing, but the difference was not statistically significant (0.056), and cold testing had greater sensitivity and higher Youden index. Clinically, LSCI thus seems best supported as a complementary physiological information, and not as a standalone test to replace history and sensibility testing [3].

Perhaps the strongest clinical argument for that complementary role is given in Figure 1. The AUC value of the conventional model with cold-response duration and EPT is already 0.8704, and the addition of LSCI recovery index raised the AUC to 0.9568, which was an increase of 0.0864. The paired DeLong comparison was significant ($p = 0.0438$), and model fit was significantly better by likelihood-ratio testing ($\chi^2 = 17.516$, $p = 0.0000285$), with LSCI remaining an independent predictor of SIP after adjustment for both sensibility tests ($p = 0.0111$). The 2025 meta-analysis by Sabharwal et al. is a useful counterpoint. While individual pulse-oximetry studies could have high diagnostic performance, the pooled result of the latter found a sensitivity of 0.92, a specificity of 0.08, an AUC of 0.62 and a DOR of 0.94. These inconsistent findings illustrate that simply being vascular does not mean being diagnostic superior and the importance of the effect of case definitions, reference standards and analytical methods on the observed accuracy. This means that the improvement shown in Figure 1 is only indicative for the current standardized LSCI protocol and does not guarantee that the same improvement will be observed for every circulation-based pulp test [27].

The incremental model in Figure 1 is also compatible with clinical practice in Europe as it stands today. The European Society of Endodontology S3 guideline highlights the importance of detailed history taking, clinical evaluation, diagnostic testing and integrated case assessment when dealing with pulpal health and diseases, rather than relying on absolute numbers. Of note, the LSCI is not yet a standard diagnostic test in that guideline. This difference needs to be considered when interpreting the present study. The higher value of AUC 0.9568 compared to 0.8704 from the model with cold duration and EPT indicates that the extended model provides additional information which is not fully captured with cold duration and EPT measurements alone, but further external validation is needed before this model can be used for a clinical decision algorithm. Its most likely future would be in diagnostically questionable vital teeth, as an objective physiology adjunct to, but not a replacement for, the patient's history, cold testing, percussion and radiographic and operative findings. This multimodal interpretation is more in line with current clinical recommendations rather than a threshold approach to determine treatment [28].

The improvement in Figure 1 can also be put into perspective with the development of molecular biomarkers. Nawal and coworkers have measured the concentration of IL-8 and TNF-α in the pulps of teeth with reversible and irreversible pulpitis as well as in their blood. IL-8 had an AUC of 0.997 (with 95.5% sensitivity and 99.76% specificity) while TNF-α had an AUC of 0.812 (59.1% sensitivity and 92.1% specificity). These results provide strong justification for the presumption of the current study, which is that objective biological measurements can differentiate inflammatory states other than traditional subjective assessments. Although the AUC of the current extended model was 0.9568, it was yet outperformed by the IL-8 model. Pulpal cytokines cannot be used as a completely noninvasive preoperative test because blood needs to be sampled from the pulp after exposure. LSCI, however, questions physiology in the whole tooth. Thus, the two methods shouldn't be seen as rivals, but molecular biomarkers could serve as a wonderful standard for future research to assess whether abnormal recovery of LSCI is a good indicator of inflammatory burden [8].

And that's another reason why the incremental improvement in Figure 1 is possibly of clinical significance, Richert and colleagues say. They pointed out that the reversible/irreversible distinction is a clinical therapeutic classification that does not necessarily reflect the complex biology that occurs at the cell and tissue level in pulpitis. They emphasized the need for models and diagnostic approaches that more closely reflect the spectrum of pulp inflammation and repair. The current study addresses that issue by quantifying a continuous, physiological phenotype, as opposed to simply asking whether a patient feels pain or whether they can sense an electrical stimulus. However, the same biological continuum cautions against using the 0.0709 LSCI threshold as an absolute biological threshold. This is an empirically useful ROC cutoff; it is not an indication that all values below are recoverable tissue, and all values above are irreversible. The more defensible interpretation of Figure 1 is that the dynamic vascular information is used to enhance discrimination in a multimodal probabilistic model [29].

Figure 1 should be interpreted in the light of practical limitations identified for other optical vascular tests. Kasper et al. screened 38 publications that covered dental pulse oximetry and concluded that challenges with maintaining optimal emitter/detector geometry, optical diffraction through enamel, dentin and gingiva, differences in patient age, and a lack of dental-specific instruments were the largest hurdles. Such restrictions are very significant because any optical pulp test is susceptible to the tissues located between the vascular source and the detector. Several of these issues were overcome in the present study by using a fixed transillumination geometry, by using an individualized stabilization, and by using locked camera parameters and within-tooth baseline normalization. The methodological standardization might be a partial answer to why the inclusion of LSCI index in the model enhanced it, because of known issues with dental optical measurements. Differences in crown morphology, dentin thickness, restorations and optical access are, however, possible sources of external variability. For clinical implementation, therefore, simplified positioning hardware, as well as automated quality control and prospective testing in less selected populations would have to be performed before the impressive Figure 1 result could be assumed to be repeatable outside the research setting [30].

Biological validation independent of the diagnostic-group comparison is provided in figure 2. In the 22 SIP teeth with available histology, the LSCI recovery index was found to have a positive correlation with the severity of the histopathology (Spearman $\rho = 0.551$, $p = 0.00788$), with higher central values in the mild, moderate and severe disease groups. The relationship is clinically meaningful but is not deterministic and there is a visible spread within each grade. Contreras and colleagues independently examined reversible and symptomatic irreversible pulpitis via immunohistology and determined that neutrophilic involvement (increased density, increased activity of neutrophil extracellular trap) was significantly greater in the group with symptomatic irreversible pulpitis. Their findings corroborate the trajectory of the current partnership as they found that as inflammatory severity increases there are measurable tissue-level changes that can impinge local microvascular regulation. The present study lends a clinically appealing twist: the persistence of the post-cold vascular response could serve as a functional noninvasive marker of the inflammatory burden [5].

The moderate not near perfect correlation in figure 2 is also consistent with what was observed by Raoof and others. Of 75 carious molars and three sound controls, the acute inflammation and hyperemia, as well as pulp exposure, were significantly more likely to be seen in teeth clinically diagnosed as being irreversible pulpitis, while fibrosis was more likely to be seen in the reversible group. However, several other histopathologic variables (overall inflammation severity, necrosis) did not differ significantly among groups, and the authors clearly gave the noted differences between clinical,

radiographic and histopathologic diagnosis. Their findings lend support and a qualification for the present study. They confirm the association of vascular and inflammatory changes with more advanced clinical disease including hyperemia but state that no single clinical or physiological measurement can be expected to give a perfect reflection of the histology. A Spearman correlation of 0.551 is biologically plausible because LSCI measures a single dimension (microvascular recovery), and the severity of the histology also involves spatially heterogeneous inflammation, necrosis, fibrosis, distribution of bacteria, and reparative responses, which cannot be summarized in a single perfusion index [4].

Ricucci and co-authors also offer especially solid histopathologic evidence for a link between vascular dysfunction and late stage, symptomatic pulpitis. All the 32 teeth with untreated deep caries and symptomatic irreversible pulpitis showed severe acute inflammation, necrosis in the pulp chamber, microabscess and bacterial infection of the pulp, and bacterial penetration in the blood vessels of the pulp in all teeth. Such observations provide a reasonable tissue level explanation for the highest LSCI recovery indices in the severe histologic grade in Figure 2. It is logical that vascular congestion, focal necrosis, microabscess formation and direct involvement of blood vessels could have a negative impact on the ability of the remaining functioning microcirculation to quickly return to its baseline state following cold provocation. The present study cannot determine that the abnormal LSCI trajectory was due to bacterial vascular invasion, as microbiological vascular invasion was not directly measured. However, the strong association of the physiologic signal with known vascular disease of SIP provides significant added biological plausibility for the relationship and further encourages studies correlating LSCI with detailed histobacteriology [31].

A significant clinical corollary is that more extensive and/or more abnormal histology or physiology does not necessarily equate with the absence of any remaining vital pulp tissue. Taha et al. randomly assigned 60 mature molars with irreversible pulpitis to two groups: full pulpotomy or root-canal treatment and found 27 out of 29 (93%) in each group to be successful at 12 months. Pulpotomy also resulted in less pain, less use of analgesics and quicker alleviation of pain on the first day. These findings contradict the literal meaning of the word "irreversible" in the word of the tooth and suggest that the entire tooth does not have to be irreparable. They are thus very relevant to Figure 2, where the positive LSCI–histology correlation confirms that the recovery index reflects increasing disease burden; however, this correlation does not automatically set a threshold for pulpectomy or root-canal therapy. This is further illustrated by the scatter seen in the severe histologic group. From a clinical perspective, the future use of LSCI could eventually be used to quantify the extent of the inflammation and help select treatment, however, therapeutic thresholds would have to be correlated to outcomes following vital pulp therapy and based on the diagnosis rather than simply correlated to diagnosis [32].

Conclusion

A clear difference in the microvascular recovery of the pulps after cold challenge using LSCI was found between reversible pulpitis and symptomatic irreversible pulpitis. While the optical signal quality was similar at baseline, the vascular disturbance was greater and lasted longer with SIP, and the T50 and T90 were significantly increased and the return to baseline was slower. The prespecified microvascular recovery index had a good diagnostic discrimination value (AUC 0.9088, specificity 96%, positive likelihood ratio 18.0). Importantly, the diagnostic value was not confined to the use of LSCI alone in comparison to conventional tests, as the addition of LSCI index to cold-response duration and EPT improved the model AUC from 0.8704 to 0.9568 and significantly improved overall model fit.

The good correlation between the incremental histopathologic grade and the LSCI recovery index also provided further evidence that the vascular abnormality measured is biologically relevant, and the good inter-analyst reproducibility suggested that the analytical procedure could be applied in a standardized manner. The success of the reversible-pulpitis teeth that were clinically and vitality confirmed at 6 months further supported the reference classification. All these findings are in favor of dynamic microvascular recovery after a standard cold challenge as a physiologically meaningful indicator of pulpal inflammatory status. Cold challenge transillumination LSCI is thus a potentially valuable objective adjunct in a conventional sensibility testing paradigm to distinguish RP from SIP, especially when there is diagnostic confusion based on the symptoms alone. Larger independent and multicenter studies are needed to further validate the proposed recovery index and operating cutoff prior to routine clinical use.

References

1. Karrar, R. N., Craig, S. G., Duncan, H. F., Abushouk, S. A., Elfiel, S. Y., Lundy, F. T., Clarke, M., El-Karim, I. A., & Reliability Assessment Group. (2025). Clinical validation of a proposed diagnostic classification for pulpitis. *International Endodontic Journal, 58*(8), 1158–1171. https://doi.org/10.1111/iej.14254

2. Kahler, B., Taha, N. A., Lu, J., & Saoud, T. M. (2023). Vital pulp therapy for permanent teeth with diagnosis of irreversible pulpitis: Biological basis and outcome. *Australian Dental Journal, 68*(S1), S110–S122. https://doi.org/10.1111/adj.12997

3. Donnermeyer, D., Dammaschke, T., Lipski, M., & Schäfer, E. (2023). Effectiveness of diagnosing pulpitis: A systematic review. *International Endodontic Journal, 56*(Suppl. 3), 296–325. https://doi.org/10.1111/iej.13762

4. Raoof, M., Vazavandi, E., Torabi Parizi, M., Hatami, N., Mohammadalizadeh, S., Amanpour, S., & Haghani, J. (2022). Clinical, radiological, and histological correlation in diagnosis of pulpitis. *Dental Research Journal, 19*, 25. https://doi.org/10.4103/1735-3327.340110

5. Contreras, C., Cádiz, B., & Schmachtenberg, O. (2023). Determination of the severity of pulpitis by immunohistological analysis and comparison with the clinical picture. *Journal of Endodontics, 49*(1), 26–35. https://doi.org/10.1016/j.joen.2022.10.012

6. Wahyudi, R., Aguilar, P., Changsiripun, C., Lertpimonchai, A., Samaranayake, L., Soe, Z. C., Osathanon, T., Everts, V., Limjeerajarus, C. N., & Limjeerajarus, N. (2026). Inflammatory biomarkers in irreversible pulpitis and pulp necrosis: A systematic review and meta-analysis. *International Dental Journal, 76*(2), 109453. https://doi.org/10.1016/j.identj.2026.109453

7. Karrar, R. N., Cushley, S., Duncan, H. F., Lundy, F. T., Abushouk, S. A., Clarke, M., & El-Karim, I. A. (2023). Molecular biomarkers for objective assessment of symptomatic pulpitis: A systematic review and meta-analysis. *International Endodontic Journal, 56*(10), 1160–1177. https://doi.org/10.1111/iej.13950

8. Nawal, R. R., Yadav, S., Duncan, H. F., Talwar, S., Kaushik, A., Singh, V. K., & Koner, B. C. (2024). Discriminatory performance of the pulpal inflammatory biomarkers; Interleukin-8 and TNF-α in patients with symptoms indicative of reversible and irreversible pulpitis: A diagnostic accuracy study. *International Endodontic Journal, 57*(9), 1200–1211. https://doi.org/10.1111/iej.14078

9. Li, Q. (2025). Diagnostic utility of Th2 cytokines (IL-4, IL-5, IL-10, and IL-13) in pulpal blood for assessing pulpitis severity. *BMC Oral Health, 25*(1), 527. https://doi.org/10.1186/s12903-025-05936-0

10. Muñoz, P., Ruíz-Pérez, V. H., Martínez-Martínez, A., & Alpuche, J. (2026). Rapid point-of-care quantification of high-sensitivity C-reactive protein in pulpal blood as an objective biomarker for irreversible pulpitis: A pilot diagnostic accuracy study. *Frontiers in Dental*

Medicine, 6, 1729860. https://doi.org/10.3389/fdmed.2025.1729860
11. Patro, S., Meto, A., Mohanty, A., Chopra, V., Miglani, S., Das, A., Luke, A. M., Al Hadi, D., Meto, A., Fiorillo, L., Karobari, M. I., Wahjuningrum, D. A., & Pawar, A. M. (2022). Diagnostic accuracy of pulp vitality tests and pulp sensibility tests for assessing pulpal health in permanent teeth: A systematic review and meta-analysis. *International Journal of Environmental Research and Public Health, 19*(15), 9599. https://doi.org/10.3390/ijerph19159599
12. Afkhami, F., Wright, P. P., Chien, P. Y.-H., Xu, C., Walsh, L. J., & Peters, O. A. (2024). Exploring approaches to pulp vitality assessment: A scoping review of nontraditional methods. *International Endodontic Journal, 57*(8), 1065–1098. https://doi.org/10.1111/iej.14073
13. Oo, T. D., Kakino, S., Kusano, M., Ikeda, H., Miyashin, M., & Okiji, T. (2020). Transmitted-light plethysmography detects changes in human pulpal blood flow elicited by innocuous tooth cooling and foot heating. *Archives of Oral Biology, 119*, 104881. https://doi.org/10.1016/j.archoralbio.2020.104881
14. Stoianovici, C., Wilder-Smith, P., & Choi, B. (2011). Assessment of pulpal vitality using laser speckle imaging. *Lasers in Surgery and Medicine, 43*(8), 833–837. https://doi.org/10.1002/lsm.21090
15. Xiong, W., Xia, N., Yang, Y., He, X., & Yang, J. (2025). In vitro study of pulp blood flow based on laser speckle contrast imaging. *Photodiagnosis and Photodynamic Therapy, 56*, 105227. https://doi.org/10.1016/j.pdpdt.2025.105227
16. Nemeth, L., Birk, L., Birk, L., & Cankar, K. (2022). Laser-Doppler microvascular flow of dental pulp in relation to caries progression. *Lasers in Medical Science, 37*(3), 1549–1557. https://doi.org/10.1007/s10103-021-03402-1
17. Lam, R., Goonewardene, M. S., & Naoum, S. (2020). Pulp blood flow and sensibility in patients with a history of dental trauma undergoing maxillary expansion: A prospective study. *The Angle Orthodontist, 90*(5), 695–701. https://doi.org/10.2319/022520-129.1
18. Yin, F., Zhao, J., Zhang, H., Wang, S., An, Q., Wei, X., Tang, C., & Han, S. (2025). Effect of orthodontic force on gingival blood flow measured by laser speckle contrast imaging: A randomised controlled trial. *International Dental Journal, 75*(5), 100932. https://doi.org/10.1016/j.identj.2025.100932
19. Galler, K. M., Weber, M., Korkmaz, Y., Widbiller, M., & Feuerer, M. (2021). Inflammatory response mechanisms of the dentine–pulp complex and the periapical tissues. *International Journal of Molecular Sciences, 22*(3), 1480. https://doi.org/10.3390/ijms22031480
20. Hasan, A., Roome, T., Wahid, M., Ansari, S. A., Akhtar, H., Jilani, S. N. A., & Kiyani, A. (2022). Gene expression analysis of toll like receptor 2 and 4, Dectin-1, Osteopontin and inflammatory cytokines in human dental pulp ex-vivo. *BMC Oral Health, 22*(1), 563. https://doi.org/10.1186/s12903-022-02621-4
21. Wang, J., Qiao, J., Ma, L., Li, X., Wei, C., Tian, X., & Liu, K. (2023). Identification of the characteristics of infiltrating immune cells in pulpitis and its potential molecular regulation mechanism by bioinformatics method. *BMC Oral Health, 23*(1), 287. https://doi.org/10.1186/s12903-023-03020-z
22. Wang, B., Li, W., Huang, W., Li, X., Li, J., Shi, S., Mao, X., & Wei, X. (2025). Multiple cell death modalities and immune response in pulpitis. *International Endodontic Journal, 58*(1), 111–127. https://doi.org/10.1111/iej.14145
23. Demant, S., Dabelsteen, S., & Bjørndal, L. (2021). A macroscopic and histological analysis of radiographically well-defined deep and extremely deep carious lesions: Carious lesion characteristics as indicators of the level of bacterial penetration and pulp response. *International Endodontic Journal, 54*(3), 319–330. https://doi.org/10.1111/iej.13424
24. Molaasadolah, F., Zargar, N., Bargrizan, M., Akbari, F., Kardouni Khozestani, P., Sabour, S., & Bakhshi, M. (2022). Comparison of pulse oximeter, cold test, and electric pulp test for assessment of pulp vitality in permanent immature teeth. *Folia Medica, 64*(1), 134–142. https://doi.org/10.3897/folmed.64.e66573
25. Gupta, D., Shaw, A. K., Gaikwad, A., Kale, P., Deshpande, S. M., & Gachake, A. (2025). The diagnostic accuracy of pulse oximetry for assessing pulp vitality: A systematic review. *Cureus, 17*(1), e76820. https://doi.org/10.7759/cureus.76820
26. Zeb Jan, M., Zakir, S., Ali, A., Nayab, R., Mehmood, A., & Khan, I. U. (2023). Diagnostic accuracy of cold test and electric pulp testing for testing pulp vitality in single rooted teeth with irreversible pulpitis. *Journal of Khyber College of Dentistry, 13*(1), 13–16. https://doi.org/10.33279/jkcd.v13i1.32
27. Sabharwal, R. J., Dhull, K. S., Dutta, B., Devraj, I. M., Surana, P., Misra, A., & Gupta, A. (2025). Evaluation of pulp vitality using pulse oximetry: A systematic review and meta-analysis. *International Journal of Clinical Pediatric Dentistry, 18*(4), 479–486. https://doi.org/10.5005/jp-journals-10005-3107
28. Duncan, H. F., Kirkevang, L.-L., Peters, O. A., El-Karim, I., Krastl, G., Del Fabbro, M., Chong, B. S., Galler, K. M., Segura-Egea, J. J., Kebschull, M., & ESE Workshop Participants and Methodological Consultant. (2023). Treatment of pulpal and apical disease: The European Society of Endodontology (ESE) S3-level clinical practice guideline. *International Endodontic Journal, 56*(Suppl. 3), 238–295. https://doi.org/10.1111/iej.13974
29. Richert, R., Ducret, M., Alliot-Licht, B., Bekhouche, M., Gobert, S., & Farges, J.-C. (2022). A critical analysis of research methods and experimental models to study pulpitis. *International Endodontic Journal, 55*(Suppl. 1), 14–36. https://doi.org/10.1111/iej.13683
30. Kasper, R. H., Coelho, M. R., Miguens-Jr, S. A. Q., Grazziotin-Soares, R., & Barletta, F. B. (2024). Pulse oximetry as a dental pulp test: A scoping review to identify barriers hindering the use of oximeters in clinical practice. *The Saudi Dental Journal, 36*(2), 262–269. https://doi.org/10.1016/j.sdentj.2023.11.006
31. Ricucci, D., Siqueira, J. F., Jr., Abdelsayed, R. A., Lio, S. G., & Rôças, I. N. (2021). Bacterial invasion of pulp blood vessels in teeth with symptomatic irreversible pulpitis. *Journal of Endodontics, 47*(12), 1854–1864. https://doi.org/10.1016/j.joen.2021.09.010
32. Taha, N. A., Abuzaid, A. M., & Khader, Y. S. (2023). A randomized controlled clinical trial of pulpotomy versus root canal therapy in mature teeth with irreversible pulpitis: Outcome, quality of life, and patients' satisfaction. *Journal of Endodontics, 49*(6), 624–631.e2. https://doi.org/10.1016/j.joen.2023.04.001

Vol 14, No 3 (2026) DOI 10.5195/d3000.2026.1665

Table 1. Baseline demographic, clinical, radiographic, and conventional pulp-test characteristics of the study groups.

Variable	RP (n=25)	SIP (n=25)	Test statistic	Effect estimate (95% CI)	p-value
Age (years)	36.88 ± 7.2	38.81 ± 8.17	Welch t=0.8852, df=47.26	Δ=1.928 (−2.453 to 6.309); g=0.246	0.3805
Female sex	13/25 (52%)	14/25 (56%)	Fisher exact	OR=1.175 (0.386–3.576)	1
Maxillary arch	12/25 (48%)	13/25 (52%)	Fisher exact	OR=1.174 (0.387–3.56)	1
First molar	16/25 (64%)	15/25 (60%)	Fisher exact	OR=0.844 (0.269–2.647)	1
Spontaneous pain	2/25 (8%)	18/25 (72%)	Fisher exact	OR=29.571 (5.466–159.975)	6.30991×10^{-6}
Nocturnal pain	1/25 (4%)	15/25 (60%)	Fisher exact	OR=36 (4.175–310.453)	3.40241×10^{-5}
Lingering thermal pain	3/25 (12%)	22/25 (88%)	Fisher exact	OR=53.778 (9.766–296.137)	8.51293×10^{-8}
Percussion sensitivity	4/25 (16%)	14/25 (56%)	Fisher exact	OR=6.682 (1.768–25.246)	0.00715037
Radiographic caries-to-pulp distance (mm)	0.61 ± 0.21	0.52 ± 0.17	Welch t=−1.7349, df=45.78	Δ=−0.095 (−0.205 to 0.015); g=−0.483	0.08948
Cold-response duration (s)	6.8 [5.2–7.9]	17.8 [10.5–22.7]	Mann–Whitney U=92	Rank-biserial r=0.7056	1.96138×10^{-5}
EPT threshold (0–64)	24 ± 8.5	26.68 ± 5.86	Welch t=1.2971, df=42.61	Δ=2.68 (−1.488 to 6.848); g=0.361	0.2016

Table 2. Cold-challenge Laser speckle contrast imaging signal quality and primary/secondary microvascular recovery parameters.

Parameter	RP (n=25)	SIP (n=25)	Test statistic	Effect estimate (95% CI)	p-value
Baseline SFI coefficient of variation (%)	5.07 ± 1.03	5.48 ± 1.18	Welch t=1.3335, df=47.15	Δ=0.42 (−0.21 to 1.05); g=0.371	0.1888
Rejected frames (%)	2.22 ± 0.83	1.76 ± 0.98	Welch t=−1.7687, df=46.72	Δ=−0.46 (−0.97 to 0.06); g=−0.492	0.08347
Immediate absolute change from baseline (%)	20.03 ± 5.34	23.1 ± 5.1	Welch t=2.0738, df=47.9	Δ=3.06 (0.09–6.03); g=0.577	0.0435
Dominant early absolute excursion (%)	20.83 ± 5.47	23.56 ± 5.21	Welch t=1.8059, df=47.89	Δ=2.73 (−0.31 to 5.77); g=0.503	0.07721
Primary microvascular recovery index	0.0444 ± 0.019	0.094 ± 0.0325	Welch t=6.5874, df=38.68	Δ=0.0496 (0.0343–0.0648); g=1.834	8.23615×10^{-8}
T50 (s)	36.9 ± 11.9	69.8 ± 18	Welch t=7.6281, df=41.63	Δ=32.96 (24.24–41.68); g=2.124	1.96884×10^{-9}
T90 (s)	72 [52–89]	132 [111–162]	Mann–Whitney U=39.0	Rank-biserial r=0.8752	1.16186×10^{-7}
Recovery slope, 10–90 s (SFI units/s)	−0.002103 ± 0.000662	−0.001725 ± 0.000526	Welch t=2.2339, df=45.66	Δ=0.000378 (0.000037–0.000718); g=0.622	0.03043
Absolute deviation recovery-curve area (SFI·s)	8 ± 3.42	16.92 ± 5.84	Welch t=6.5874, df=38.68	Δ=8.92 (6.18–11.66); g=1.834	8.23615×10^{-8}

Vol 14, No 3 (2026) DOI 10.5195/d3000.2026.1665

Table 3. Mixed-effects analysis of the 180-second normalized pulpal microvascular recovery trajectory.

Global model effects

Model effect/statistic	Wald χ^2 / value	df	p-value
Diagnostic group: SIP vs RP	45.0711	1	1.90012×10^{-11}
Time, natural cubic spline	35,664.8934	4	$5.2244411432\times10^{-7741}$
Diagnosis × time interaction	3,318.0804	4	$5.10633084675\times10^{-718}$
Random-intercept variance	0.000682	—	—
Residual variance	0.000465	—	—
Marginal R^2	0.8123	—	—
Conditional R^2	0.9239	—	—
AIC	−43,454.757	—	—
BIC	−43,369.431	—	—

Model-estimated recovery trajectory

Time	RP estimated SFI	SIP estimated SFI	SIP−RP difference	95% CI	z	p-value
0 s	0.7904	0.7647	−0.0257	−0.0406 to −0.0108	−3.3811	0.00072199
30 s	0.8868	0.8198	−0.0671	−0.0817 to −0.0525	−9.019	1.89831×10^{-19}
60 s	0.9564	0.8728	−0.0836	−0.0981 to −0.0690	−11.2426	2.51982×10^{-29}
90 s	0.9904	0.9204	−0.07	−0.0846 to −0.0554	−9.3982	5.54813×10^{-21}
120 s	0.9994	0.9576	−0.0418	−0.0564 to −0.0272	−5.6245	1.86050×10^{-8}
180 s	1.0002	0.9976	−0.0026	−0.0175 to 0.0123	−0.3418	0.7325

Table 4. Diagnostic accuracy of the prespecified microvascular recovery index and conventional pulp sensibility tests.

Diagnostic performance

Index test	AUC (95% bootstrap CI)	p vs AUC=0.50	Youden cutoff	Sensitivity (95% CI)	Specificity (95% CI)	LR+ (95% CI)	LR− (95% CI)	Youden J
LSCI recovery index	0.9088 (0.8192–0.976)	8.89665×10^{-24}	0.0709	0.72 (0.524–0.857)	0.96 (0.805–0.993)	18 (2.597–124.745)	0.292 (0.155–0.55)	0.68
Cold-response duration	0.8528 (0.7248–0.9568)	5.37748×10^{-9}	9.9 s	0.84 (0.653–0.936)	0.88 (0.7–0.958)	7 (2.389–20.515)	0.182 (0.073–0.452)	0.72
EPT threshold	0.6056 (0.4416–0.7648)	0.20179	25	0.68 (0.484–0.828)	0.6 (0.407–0.766)	1.7 (0.981–2.947)	0.533 (0.277–1.027)	0.28

Pairwise comparison of correlated AUCs

Comparison	AUC difference	95% CI	z	p value
LSCI vs cold-response duration	0.056	−0.084 to 0.196	0.7838	0.43313
LSCI vs EPT	0.3032	0.1301 to 0.4763	3.4327	0.00059768
Cold-response duration vs EPT	0.2472	0.0514 to 0.443	2.4747	0.0133355